

# Air-to-Water Cascade Heat Pump Thermal Performance Modelling for Continental Climate Regions

## Modélisation des performances thermiques d'une thermopompe air-eau en cascade pour les climats continentaux froids

Ye. Yerdesh<sup>1,2</sup>, A. Toleukhanov<sup>1,2</sup>, M. Mohanraj<sup>3</sup>, H.S. Wang<sup>4</sup>, O. Botella<sup>5</sup>, M. Feidt<sup>5</sup>, Ye. Belyayev<sup>1,2\*</sup>

<sup>1</sup> Department of Mechanics, Al-Farabi Kazakh National University, Almaty, Kazakhstan

<sup>2</sup> Department of Mechanical Engineering and Modeling, Satbayev University, Almaty, Kazakhstan

<sup>3</sup> Department of Mechanical Engineering, Hindusthan College of Engineering and Technology, Coimbatore, India

<sup>4</sup> School of Engineering and Materials Sciences, Queen Mary University of London, UK

<sup>5</sup> Université de Lorraine, CNRS, LEMTA, F-54000 Nancy, France

Corresponding author: [yerzhan.belyayev@gmail.com](mailto:yerzhan.belyayev@gmail.com)

**ABSTRACT.** At low ambient temperatures, the heating capacity and coefficient of performance of a single stage vapour compression heat pump cycle is significantly getting reduced. A two-stage cascade heat pump cycle operating with two different refrigerants provides a sustainable solution to lift the condenser temperature above 70 °C. Calculation of thermal performance for various refrigerants pairs has been carried out by using Engineering Equation Solver software. The following refrigerants pairs R410A/R290, R410A/R1234yf, R410A/R134a, R410A/R407C, R32/R290, R32/R1234yf, R32/R134a, R32/R407C, R404A/R290, R404A/R1234yf, R404A/R134a, R404A/R407C, R744/R290, R744/R1234yf, R744/R134a, R744/R407C for low and high-temperature cycles have been tested numerically. R32/R134a and R410A/R134a shows the highest vapour compression cycle COP 1.98 from -30 °C ambient air temperature and +60 °C heating circuit temperature range, but they will be eventually suppressed in near future by Paris Agreement. As an environmentally friendly alternative to the previous pairs in the cascade cycle, R32/R290 and R744/R290 working fluids combinations are proposed.

**RÉSUMÉ.** Lorsque la température ambiante est basse, la capacité de chauffage et la performance d'une pompe à chaleur à compression de vapeur à un étage sont considérablement réduits. Une pompe à chaleur en cascade à deux étages qui fonctionne avec deux réfrigérants distincts fournit une solution durable pour élever la température du condenseur au-dessus de 70 °C. Le calcul des performances thermiques pour différentes paires de réfrigérants a été effectué à l'aide du logiciel « Engineering Equation Solver ». La performance des paires de réfrigérants suivantes : R410A/R290, R410A/R1234yf, R410A/R134a, R410A/R407C, R32/R290, R32/R1234yf, R32/R134a, R32/R407C, R404A/R290, R404A/R1234yf, R404A/R134a, R407C, R744/R290, R744/R1234yf, R744/R134a, R744/R407C pour les cycles de basse et haute température a été évaluée numériquement. Pour une température d'air ambiant aussi basse que -30 °C, et une température du circuit de chauffage de +60 °C, les paires R32/R134a et R410A/R134a présentent le cycle de compression de vapeur le plus élevé (COP 1,98), mais ils devraient être à terme supprimés par l'Accord de Paris. Une alternative respectueuse de l'environnement est représentée par les paires de réfrigérant R32/R290 et R744/R290.

**KEYWORDS.** Cascade Heat Pump, Continental Climate, Refrigerant Pairs, Thermodynamic Calculation, COP, Quality Factor, Pressure Ratio, Environmentally Friendly Working Fluid.

**MOTS-CLÉS.** Thermopompe à Cascade, Climat Continental, Paires de Réfrigérants, Calculs Thermodynamiques, COP, Facteur de Qualité, Rapport de Pression, Réfrigérants Respectueux de l'Environnement.

## 1. Introduction

Today, there is a lot of interest in cascade heat pumps for cold climate regions [YER 20]. The serial connection of two vapor compression cycles of the heat pump allows to significantly increasing the temperature range between the source evaporator and the sink condenser. As the temperature range has increased, it has become possible to use heat pump for low outdoor air temperatures (cold climates) or high temperatures of useful heat (industry with high temperature

needs). At the same time, the electricity consumption for a two-stage cascade system has significantly increased, which affects the *COP*.

Research on this topic has increased significantly over the past two-three years [BOA 21, LI 21, ZOU 20, WU 21, ZHA 21, LE 19]. For example, in [BAO 21] the performance characteristics of a water-to-water cascade multi-functional heat pump designed to provide heating, hot water, and simultaneous heating and hot water during the winter season are analyzed according to variation in secondary fluid temperature. According to [BAO 21] cascade multi-functional heat pumps have the potential to provide better energy efficiency at higher heating and hot water loads, and can, therefore, be used for simultaneous space heating and hot water generation in winter seasons. As another example, in [ZHA 21] investigates a R134a/CO<sub>2</sub> cascade air source heat pump system under China cold regions. According to their experimental results, the proposed R134a/CO<sub>2</sub> air source heat pump can supply water above +50 °C with high *COP* up to 3.07 and 1.60 when the ambient air temperature is -5 °C and -45 °C, respectively.

The authors of the present work have previously conducted research on the integration of solar thermal collectors with a cascade heat pump to increase its thermal performance [YER 20]. The configuration presented in [YER 20] operates in two-stage cascade mode all the time. In contrast, in the present case an air source heat pump can operate both in a two-stage cascade mode and in a conventional single-stage mode depending on the outdoor ambient air temperature. This configuration can significantly increase the *COP* of the system in continental climate conditions, in the off-season and summertime. This is achieved by switching on/off the first low-temperature cycle of the cascaded system and using an additional air source evaporator.

## 2. System Description

Continental climate is a type of climate characterized by stably hot summers, stably frosty winters. This type of climate is typical for the interior regions of the continents. The continental climate is dominant in a significant part of the territory of Russia, Ukraine, Kazakhstan, Uzbekistan, Mongolia, China, and the interior regions of the United States and Canada.

The cascade “Air-to-Water” heat pump consists of two vapor compression heat pump cycles (one using refrigerant with low boiling point and another using refrigerant with high critical temperature), which are coupled together to lift the temperature up to 80 °C. In this research work, the different refrigerants pairs are selected to numerically testing thermal performance of the cascade “Air-to-Water” heat pump. The following refrigerants pairs R410A/R290, R410A/R1234yf, R410A/R134a, R410A/R407C, R32/R290, R32/R1234yf, R32/R134a, R32/R407C, R404A/R290, R404A/R1234yf, R404A/R134a, R404A/R407C, R744/R290, R744/R1234yf, R744/R134a, R744/R407C for low and high-temperature cycles have been tested numerically. Both low and high temperature heat pump cycles consist of all basic components such as, compressor, condenser, expansion valve and an evaporator. The condenser of high temperature heat pump cycle relates to a hot water storage tank. Ethylene glycol was used as a heat transfer fluid to extract the heat from the condenser to the hot water storage tank. In addition, accessories such as liquid receivers, sealed type refrigerant driers and sight glasses were used to enhance the performance. The refrigerant pressure in the heat pump system is controlled using pressure cut-outs and the temperature of hot water is controlled using thermostats. Fig. 1 shows the proposed configuration of the cascade system. The schematic of the corresponding pressure-enthalpy diagram is depicted in Fig. 2. The system has two air ambient evaporators (see Fig. 1), which allow the heat pump to operate in the energy saving mode by switching off the low temperature cycle in the off-season and summertime. This means that at an outdoor air temperature of -5 °C and above, the system will operate in a conventional single-stage vapor compression cycle. The transition to a single-stage mode is carried out due to the three-way valves shown in Fig. 1. In the present study the system operation only in cascade mode is considered. The frosting issue of air source evaporators, especially the low-temperature cycle of the cascade system, is one of the important factors affecting the efficiency of the system. The

mechanism of frost formation on the walls of an outdoor heat exchanger is a complex physical process and there are various defrosting methods, which were discussed in the review paper of the authors [YAN 21]. The present paper proposes theoretical calculations based on fundamental thermodynamic considerations, while the frosting/defrosting is not considered in the model. Further research will be carried out on applying the defrosting modes discussed in [YAN 21] to the present cascade system, by the use of a thermal energy storage tank.

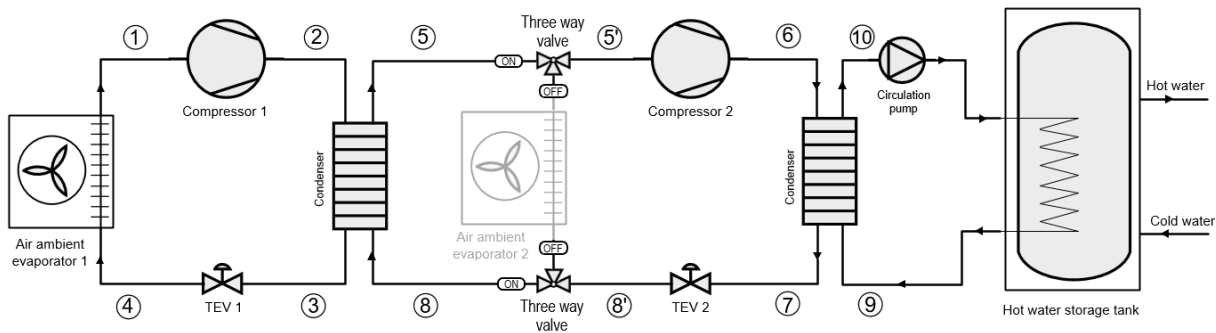


**Figure 1.** Schematic diagram of cascade air source heat pump

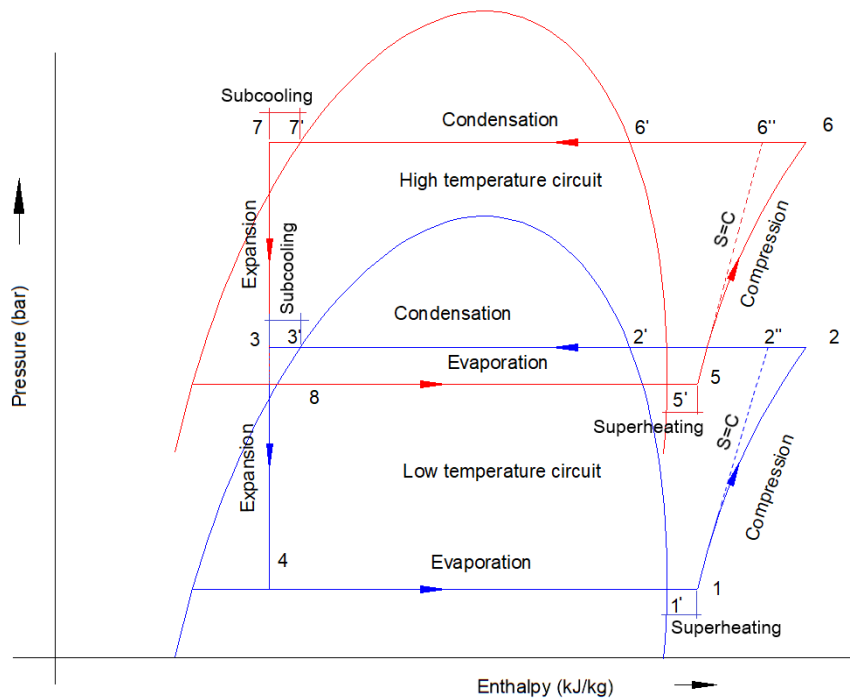


**Figure 2.** Pressure enthalpy diagram of a cascade heat pump cycle

### 3. Thermal performance modeling

The Engineering Equation Solver (EES) program [EES 18] was used to estimate the thermal characteristics of the cascade “Air-to-Water” heat pump. The initial and input parameters were chosen according to the meteorological data of Nur-Sultan, Kazakhstan. Heat output of the cascaded system was estimated using the thermo-physical properties of the refrigerant pairs presented at the end of the section. The state points 1, 2, 3 and 4 depicted in Fig. 2 represents the compressor suction, compressor discharge, condenser outlet and expansion valve outlet, respectively in the low temperature heat pump cycle. The state points 3' and 1' in Fig. 2 represent the conditions of refrigerant after sub-cooling and super heating, respectively in the low temperature heat pump cycle. Further, the state points 5, 6, 7 and 8 represents respectively the conditions of the refrigerant at the compressor suction, compressor discharge, condenser outlet and expansion valve outlet in the high

temperature heat pump cycle. The state points 7' and 5' represent the condition of refrigerant after sub-cooling and after superheating, respectively. This parameter is responsible for heat transfer. The following assumptions are considered for the modelling of the cascade ambient air source heat pump:

- (i). The refrigerant compression processes are assumed to be isentropic [MOH 18].
- (ii). The condensation of refrigerant in the condensers and evaporators of both refrigeration cycles are assumed to be constant pressure processes [MOH 18].
- (iii). The expansion of refrigerant in an expansion valve is assumed as isenthalpic [MOH 18].
- (iv). The pressure losses in the suction and discharge of both low and high temperature compressor are neglected.
- (v). Compression processes isentropic efficiencies are calculated according to [4] and [8] [SOK 81, KOS 85].
- (vi). Compressors electric motor efficiencies are assumed to be 0.85 [TRU 10].
- (vii). Compressors mechanical efficiencies are assumed to be 0.95 [TRU 10].

In addition, other model parameters such as the sub-cooling (SC) in the condenser and superheating (SH) in the evaporator, or the evaporator/condenser CAT parameters [KIM 14], will be set by the sensitivity analysis conducted in Section 4.1.

The heat gain by ambient source evaporator is given by [SON 17]:

$$\dot{Q}_{evap-LT} = \dot{m}_{ref-LT} \cdot (h_1 - h_4) \quad [1]$$

The low temperature (LT) cycle compression power is given by the following equations [TRU 10, FEI 18, MA 17]:

$$\dot{W}_{comp-LT} = \dot{m}_{ref-LT} \cdot (h_2 - h_1) \quad [2]$$

$$\dot{W}_{comp-LT} = \frac{\dot{m}_{ref-LT} \cdot (h_{2s} - h_1)}{\eta_{isen-LT}} \quad [3]$$

$$\eta_{isen-LT} = 0.98 \cdot (T_{1'} / T_{3'}) \quad [4]$$

Eq. [2] describes the actual compression 1-2 according to Fig. 2. Alternatively, Eq. [2] can be expressed in terms of Eqs [3] and [4], where the numerator of Eq. [3] describes ideal compression 1-2'' according to Fig. 2, with the assumption of adiabatic process [FEI 18]. Division by the isentropic efficiency [4] gives the actual compression [MOH 18].

The LT cycle compressor power consumption is given by:

$$\dot{W}_{elec-LT} = \frac{\dot{W}_{comp-LT}}{\eta_m \cdot \eta_t \cdot \eta_{elec}} \quad [5]$$

where  $\eta_m$  is the mechanical efficiency of the compressor, which is equal to 0.85;  $\eta_t$  is the efficiency of transmission between electric motor and compressor, where for the direct coupling it is equal to 1.0 [FEI 18];  $\eta_{elec}$  - the compressor electric motor efficiency, which is equal to 0.95.

For the high temperature (HT) cycle compression, the same approach is used as for the LT cycle [2]-[5], leading to the following formulas:

$$\dot{W}_{comp-HT} = \dot{m}_{ref-HT} \cdot (h_6 - h_5) \quad [6]$$

$$\dot{W}_{comp-HT} = \frac{\dot{m}_{ref-HT} \cdot (h_{6s} - h_5)}{\eta_{isen-HT}} \quad [7]$$

$$\eta_{isen-HT} = 0.98 \cdot (T_{5'} / T_{7'}) \quad [8]$$

$$\dot{W}_{elec-HT} = \frac{\dot{W}_{comp-HT}}{\eta_m \cdot \eta_t \cdot \eta_{elec}} \quad [9]$$

The total system power consumption is estimated using the following equation [MA 17]:

$$\dot{W}_{elec-total} = \dot{W}_{elec-HT} + \dot{W}_{elec-LT} + \dot{W}_{pump} + \dot{W}_{fan} \quad [10]$$

Heat flux for the intermediate heat exchanger working as condenser for the low temperature side is calculated as [FEI 18]:

$$\dot{Q}_{cond-LT} = \dot{m}_{ref-LT} \cdot (h_2 - h_3) \quad [11]$$

The intermediate heat exchanger for the high temperature side is used as evaporator in two-stage cascaded mode. Then, the evaporator heat flux is determined by [MA 17]:

$$\dot{Q}_{cond-LT} = \dot{Q}_{evap-HT} = \dot{m}_{ref-HT} \cdot (h_5 - h_8) \quad [12]$$

The expansion processes in an expansion device is assumed to be isenthalpic for both low and high temperature heat pump cycles. Therefore, the enthalpies before and after expansion are assumed as constant:

$$h_4 = h_3, \quad h_7 = h_8 \quad [13]$$

The useful heat condenser heating capacity is determined according to the formula:

$$\dot{Q}_{cond-HT} = \dot{m}_{ref-HT} \cdot (h_7 - h_6) \quad [14]$$

The cascaded refrigeration cycle  $COP$  is given by [MA 17]:

$$COP_{cycle} = \frac{\dot{Q}_{cond-HT}}{\dot{W}_{comp-LT} + \dot{W}_{comp-HT}} \quad [15]$$

Since heat losses in the heat exchangers of the cascaded system are not considered, the cascaded system  $COP$  is calculated according to the Equations [16]:

$$COP_{system} = \frac{\dot{Q}_{cond-HT}}{\dot{W}_{elec-total}} \quad [16]$$

The efficiency of the cascaded heat pump system in terms of the thermodynamics second law is calculated by using a quality factor  $f_q$  [FEI 18]:

$$f_q = \frac{COP_{system}}{COP_{lim}} \quad [17]$$

The limit COP associated with Carnot reverse cycle heat source and sink is determined using the following formula [FEI 18]:

$$COP_{lim} = \frac{T_{del}}{T_{del} - T_{amb}} \quad [18]$$

where  $T_{del}$  is the delivery temperature which corresponds to the heat transfer fluid at point 9 in Fig. 1, and  $T_{amb}$  is the ambient air temperature.

In addition, enthalpy and entropy values corresponding to the pressure and temperature required to calculate the system of equations [1] – [18], all thermodynamic values of the refrigerants are based on the Engineering Equation Solver (EES) software [EES 18]. For closing the system of equations [1] – [18], temperatures at the following points are determined [YER 20]:

$$T_1 = T_{amb} - CAT_{evap}, \quad T_7 = T_{del} + CAT_{cond} \quad [19]$$

The compression ratios of low temperature and high temperature cycles are given by following equations:

$$P_{ratio-LT} = \frac{p_2}{p_1}, \quad P_{ratio-HT} = \frac{p_6}{p_5} \quad [20]$$

Refrigerant	Molecular mass	Critical Temperature (°C)	Critical Pressure (MPa)	Boiling point (°C)	ASHRAE code	ODP R11 = 1	GWP 100 year
R32	52.02	78.2	5.8	-51.7	A2L	0	650
R134a	102.03	101.1	4.06	-26.1	A1	0	1430
R407C	86.2	86.4	4.63	-43.6	A1	0	1700
R410A	72.6	72.0	4.93	-51.5	A1	0	1890
R404A	97.61	72.07	3.73	-46.45	A1	0	3922
R290	44.1	96.7	4.25	-42.2	A3	0	20
R744	44.01	31.1	7.38	-78.4	A1	0	1
R1234yf	114.0	94.0	3.38	-30.0	A2L	0	4

**Table 1.** Thermodynamic properties of the refrigerants consider in this study.

The system of equations [1] - [20] is solved by the EES [EES 18] software, taking as input parameters the condenser heat flux  $\dot{Q}_{cond-HT} = 15$  kW, delivery temperature  $T_{del} = +60$  °C and varying  $T_{amb}$  ambient air temperature. The +60 °C delivery temperature was adopted in accordance with the standards in the CIS countries for a comfortable hot water supply [HVA 19]. In the next section, the results of these calculations are shown for refrigerant pairs adapted to the climate of Kazakhstan.

#### 4. Results and discussions

As mentioned above, Kazakhstan has a sharp continental climate, particularly in its capital Nur-Sultan, where the average monthly temperature is -15 °C during the heating season. On some days, the temperature may drop from -30 °C to -45 °C. Hence, for the low-temperature cycle, refrigerants with low boiling points (below -45 °C) were selected according to the data of Table 1. These

considerations led us to select the following refrigerants pairs for the low and high-temperature cycles respectively: R410A/R290, R410A/R1234yf, R410A/R134a, R410A/R407C, R32/R290, R32/R1234yf, R32/R134a, R32/R407C, R404A/R290, R404A/R1234yf, R404A/R134a, R404A/R407C, R744/R290, R744/R1234yf, R744/R134a and R744/R407C.

In order to estimate the behavior of the system efficiency parameters, we now investigate the results of the calculations obtained for the pair R32/R290. Fig. 3 displays the system efficiency parameters [15]-[18] when the ambient temperature is varied from  $-50^{\circ}\text{C}$  to  $+10^{\circ}\text{C}$ . According to this figure,  $COP_{cycle}$  is 21-23 % higher than  $COP_{system}$  in the considered temperature range. At the same time,  $f_q$  of the system is decreasing with increasing the ambient air temperature. This is because  $T_{del} = +60^{\circ}\text{C}$  is fixed, with the compression ratio decreasing accordingly as can be seen from Fig. 4. As the outside air temperature decreases, the compression ratio of the first compressor increases in the range of 3.3-21.5, while the compression ratio of the second compressor increases in the range of 2.5-5.0 (see Fig.4). For R32/R290 refrigerants, the compression ratio at  $-30^{\circ}\text{C}$  outside air temperature is 10.0 for LT cycle, and 3.8 for HT cycle.

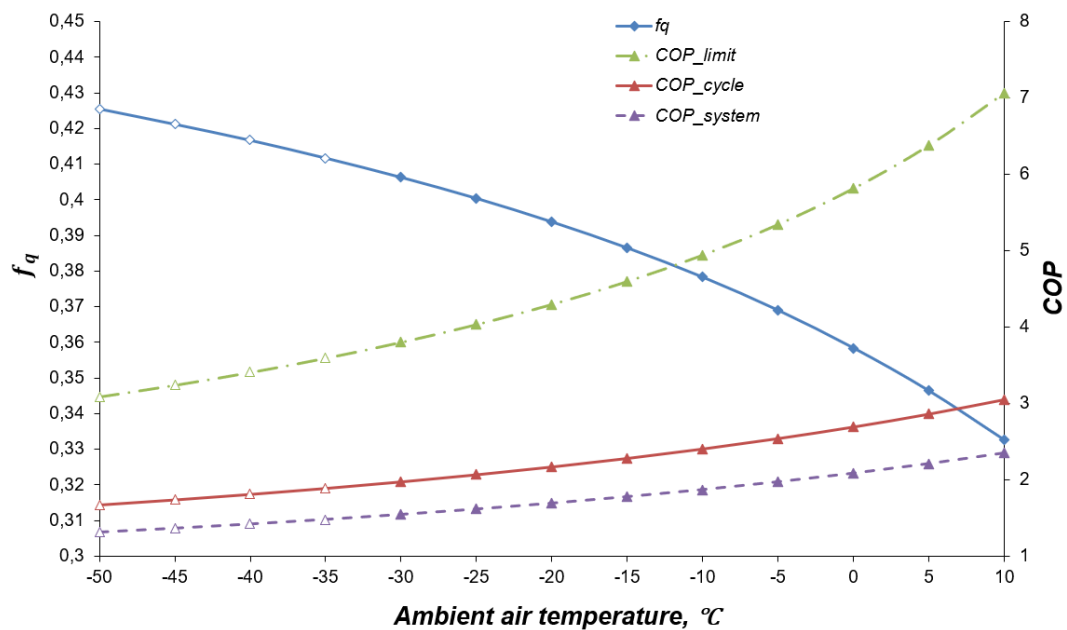


**Figure 3.** System efficiency parameters for R32/R290

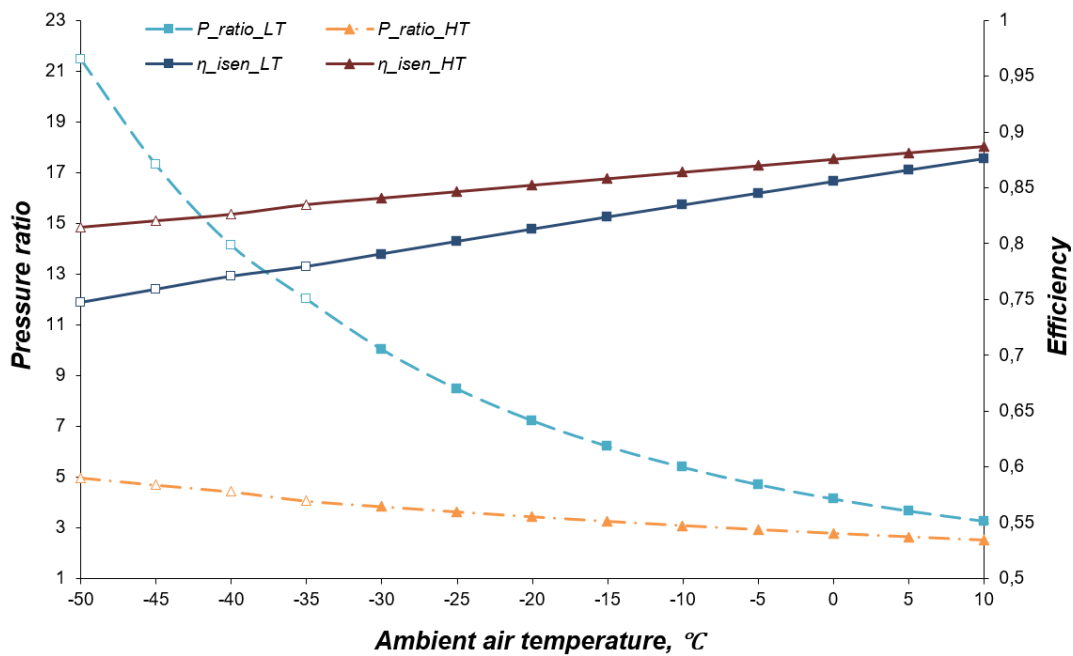


**Figure 4.** Compression process parameters for R32/R290

When the outdoor air temperature is below  $-30\text{ }^{\circ}\text{C}$ , the compression ratio of the first compressor increases significantly. At an outdoor temperature below  $-30\text{ }^{\circ}\text{C}$ , the compression ratio of the first compressor increases significantly from 10.0 to 21.5, while the isentropic efficiency of the compression process in the LT cycle decreases from 0.79 to 0.74. Since the efficiency of the compressor decreases and the risk of compressor mechanical damage increases due to operation at high compression ratios [TSO 12], as a recommendation, the figures indicate (marker) the limits of the outdoor temperature, below which the system will not work reliably.

#### 4.1. Sensitivity analysis of the model parameters

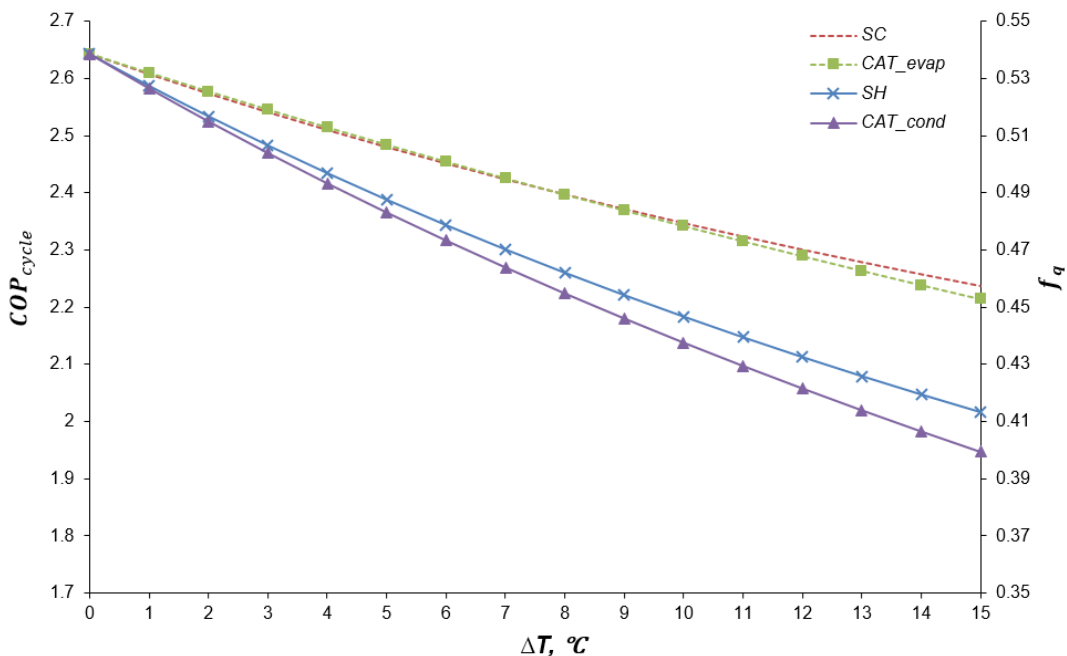


**Figure 5.** Sensitivity analysis in terms of  $COP$  and  $f_q$  for varying  $\Delta T$ .

Fig. 5 shows the sensitivity analysis for the superheating ( $SH$ ), sub-cooling ( $SC$ ), and  $CAT$  parameters. For obtaining results on the influence of parameter  $SH$ , the remaining three parameters ( $SC, CAT_{evap}, CAT_{cond}$ ) were set to zero. The results on the other parameters were obtained in a

similar fashion. According to Fig. 5, parameters  $SH$  and  $CAT_{cond}$  have the greatest influence on the system. For example, the influence of  $SH$  on the system efficiency is 35 % higher than  $SC$ . When all these parameters are set to zero, the value of  $f_q$  will be equal to 0.54. For current heat pumps and refrigeration machines, it is about 0.50 [FEI 18]. Fig. 6 shows the influence of  $SH$ ,  $SC$ ,  $CAT_{evap}$ ,  $CAT_{cond}$  on  $P_{ratio-LT}$  and  $P_{ratio-HT}$ . According to Figs 5-6,  $\Delta T$  shows the degree of increase in the coefficients  $SH$ ,  $SC$ ,  $CAT_{evap}$ ,  $CAT_{cond}$ .

According to Fig. 6, a change in parameters  $SH$ ,  $SC$ ,  $CAT_{evap}$ ,  $CAT_{cond}$  mainly affects the change in the  $P_{ratio-LT}$  of the low-temperature cycle of the cascade system. Among them, the change in  $SH$  has a greater influence. It follows from these two figures that it is not recommended to take high values for  $SH$  and  $CAT_{cond}$ . In this paper, parameters  $SH$ ,  $SC$ ,  $CAT_{evap}$ ,  $CAT_{cond}$  were taken equal to 5.0 °C.

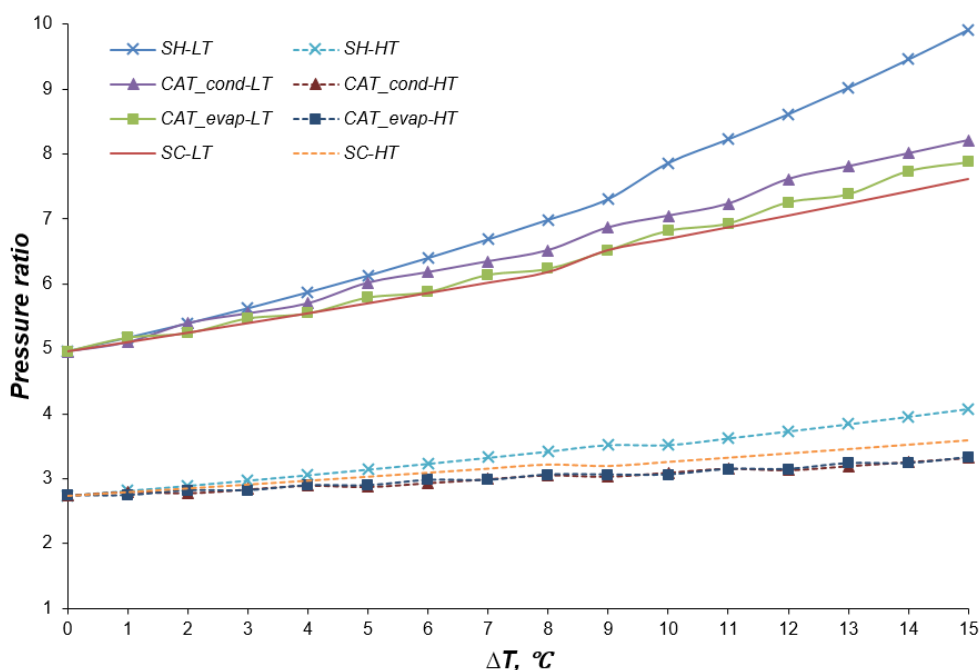


**Figure 6.** Sensitivity analysis in terms of pressure ratio for varying  $\Delta T$ .

## 4.2. Results for the various refrigerant pairs

Figs 7-10 shows a plot of  $COP$  and  $f_q$  versus ambient air temperature for the various refrigerant pairs presented in Table 1. According to these figures, the filled dots indicate the operation of the system, where the compression ratio does not exceed 10, while the unfilled dots exceed 10. Figs 7-10 allows to visually observe the dynamics of changes in the system efficiency in a wide range of outdoor air temperatures, and at the same time evaluate the limits at which the system operates reliably. Fig. 7 shows  $COP$  and  $f_q$  values for pairs with R32 used in the low temperature cycle. According to the calculations, R32/R134a and R32/R290 are the only pairs which are able to reach an ambient temperature  $T_{amb}$  below -30 °C with reasonable pressure ratio, while all other pairs can only reach  $T_{amb} = -27-28$  °C. Similarly, it can be observed from Fig.8, that the refrigerant pairs R410A/R134a and R410A/R290 reach a minimum outside temperature of -33 °C and -32 °C, respectively. According to Fig.9 R404A/R134a and R404A/R290 reach a minimum outdoor air temperature -35 °C with pressure ratio below 10. When R744 ( $CO_2$ ) is used as a working fluid in the low temperature cycle (see Fig.10), all refrigerants' pairs can reach an outdoor air temperature of -46 °C with pressure ratio below 9.0, because R744 has supercritical thermophysical properties. The

highest performance among all refrigerant's pairs can be observed for R134a and R290 as a working fluid for the second high-temperature cycle. This is because R134a and R290 have similar critical properties according to Table 1.

By comparing cascade system performance with different refrigerants pairs (Figs 7-10), R32/R134a and R410A/R134a shows the highest  $COP_{cycle}$  at  $T_{amb} = -31\text{ }^{\circ}\text{C}$ , with the value  $COP_{cycle} = 1.98$ . At  $T_{amb} = +10\text{ }^{\circ}\text{C}$  the same pairs display the highest value  $COP_{cycle} = 3.08$ , followed by the pairs R32/R290 and R410A/R290 with  $COP_{cycle} = 3.03$ . In terms of thermophysical properties and performance, R32 and R410A are close to each other. Fig.10 shows  $COP$  values for pairs with R744 used as a first refrigerant, which allows all pairs to operate as low as  $T_{amb} = -46\text{ }^{\circ}\text{C}$ . At this ambient temperature, the highest value of  $COP_{cycle}$  is reached by R744/R134a ( $COP_{cycle} = 1.67$ ), closely followed by R744/R290 with  $COP_{cycle} = 1.65$ .

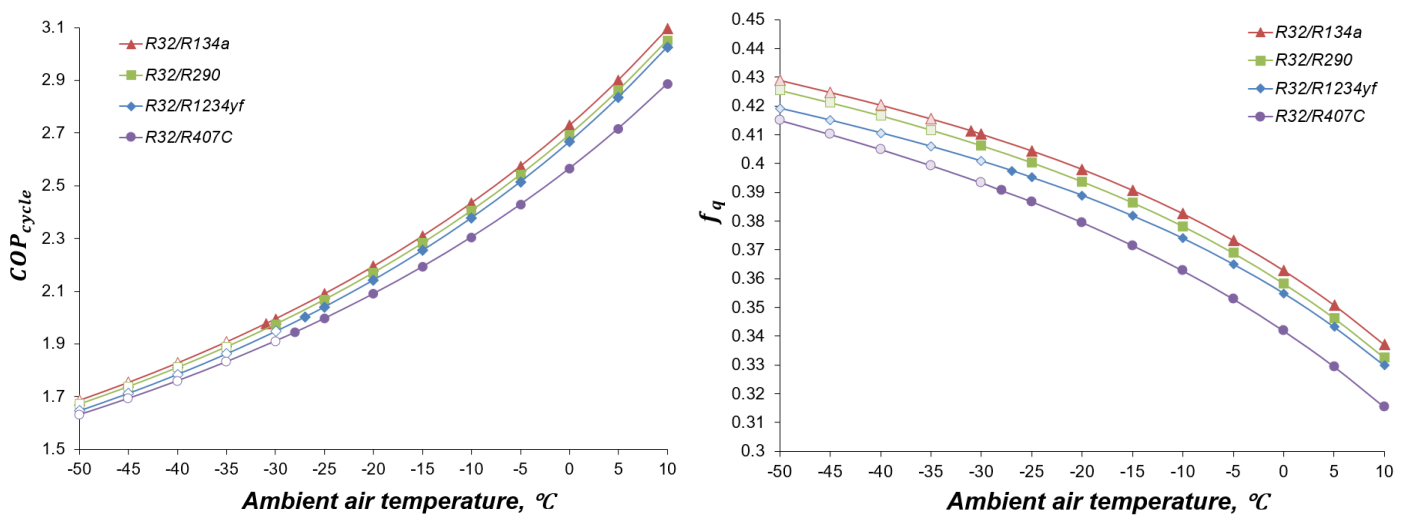


**Figure 7.** The dependence of  $COP$  (at left) and  $f_q$  (at right) on temperature of outdoor air for the different pairs with R32 for the low compression cycle.

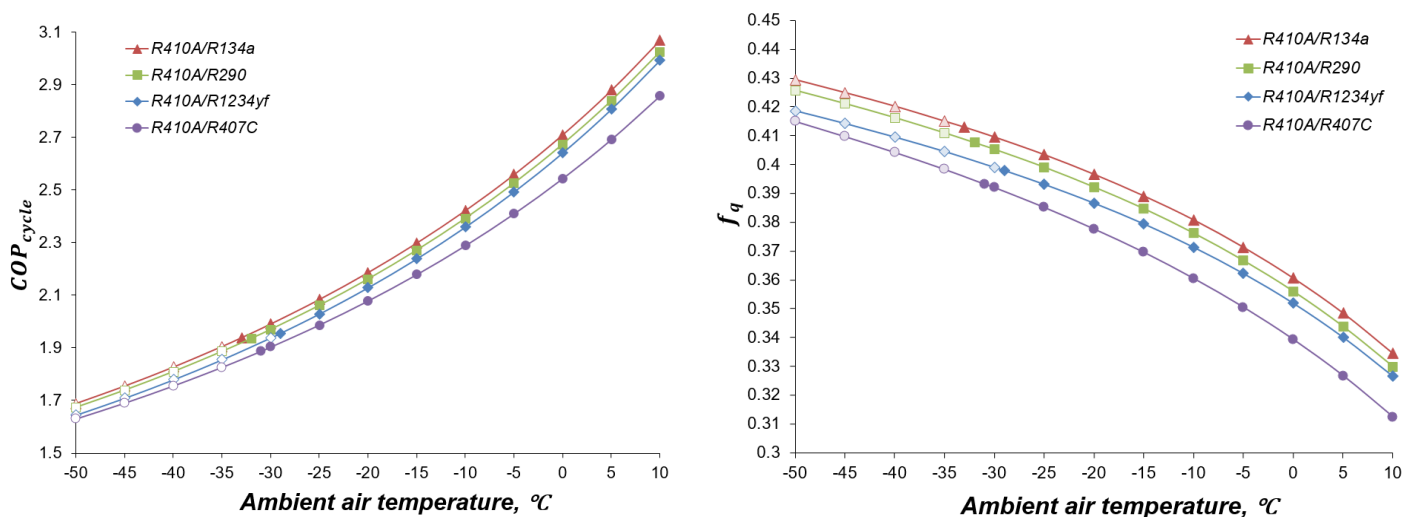


**Figure 8.** The dependence of  $COP$  (left) and  $f_q$  (right) on temperature of outdoor air for the different pairs with R410A for the low compression cycle.

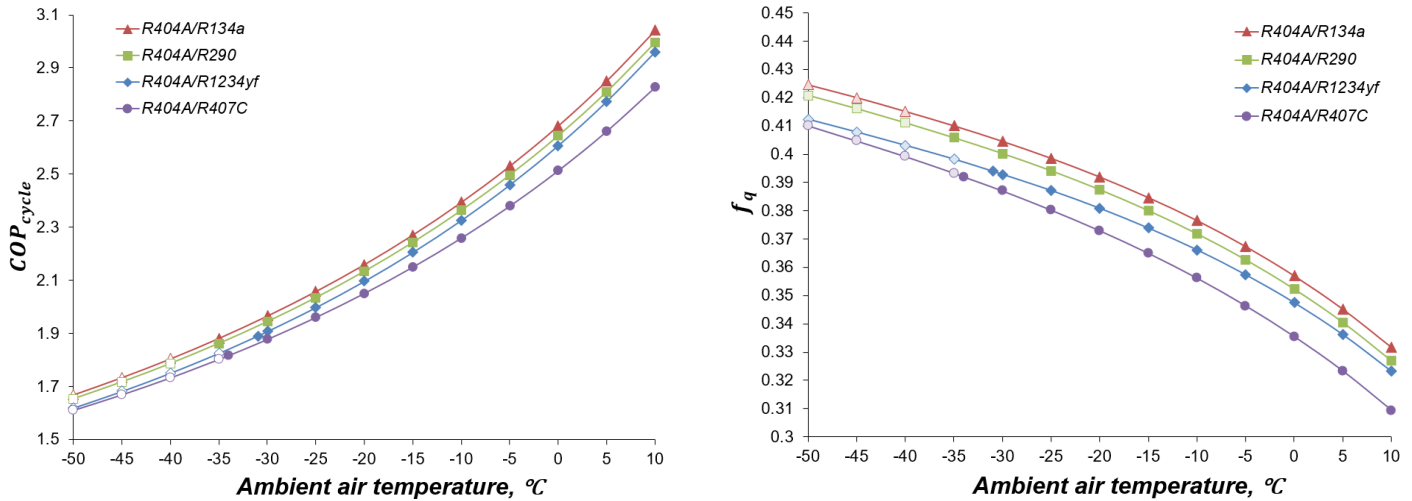


**Figure 9.** The dependence of  $COP$  (left) and  $f_q$  (right) on temperature of outdoor air for the different pairs with R404A for the low compression cycle.

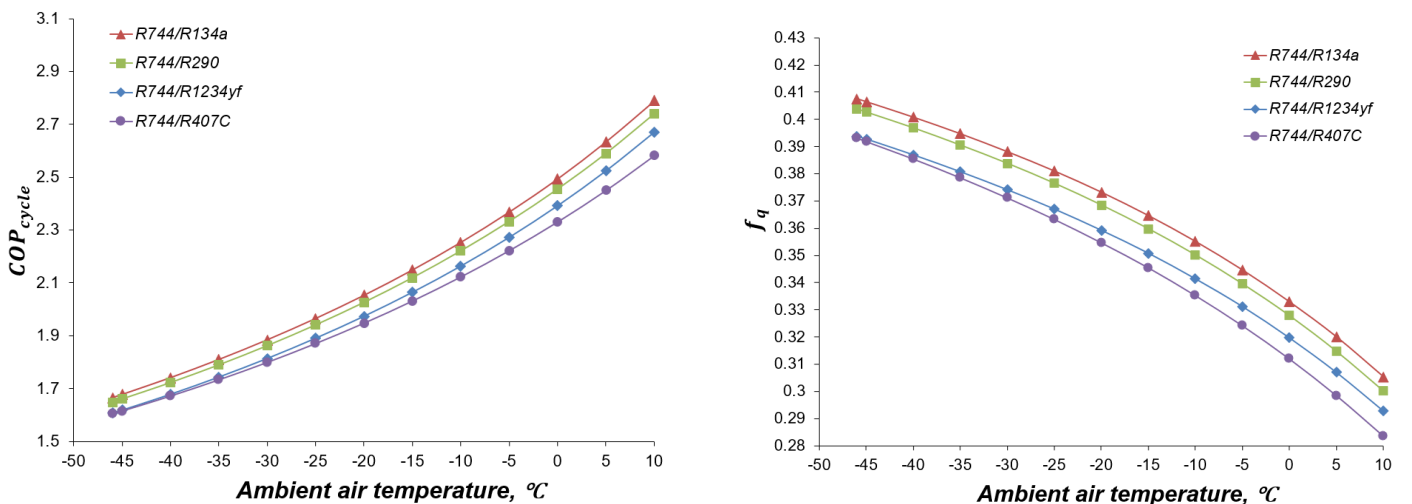


**Figure 10.** The dependence of  $COP$  (left) and  $f_q$  (right) on temperature of outdoor air for the different pairs with R744 for the low compression cycle.

The quality factor  $f_q$ , or efficiency in the sense of the second law is shown for the different refrigerant pairs according to Figs 7-10. For a heat pump,  $f_q$  is expressed as the ratio between real efficiency and efficiency of an ideal vapor compression cycle operating between  $T_{amb}$  and  $T_{del}$  (boundary conditions of reversibility) [FEI 18]. Since temperature range is decreased from  $T_{amb} = -30\text{ °C}/T_{del} = +60\text{ °C}$  to  $T_{amb} = +10\text{ °C}/T_{del} = +60\text{ °C}$   $f_q$  is decreased. The reason is a significant increase in the theoretical efficiency in the denominator of formula [18]. For example, for R32/R290 pair in outdoor air temperature range from  $-50\text{ °C}$  to  $+10\text{ °C}$   $COP_{lim} = 3.09 - 7.06$ , while  $COP_{system} = 1.32 - 2.35$ .

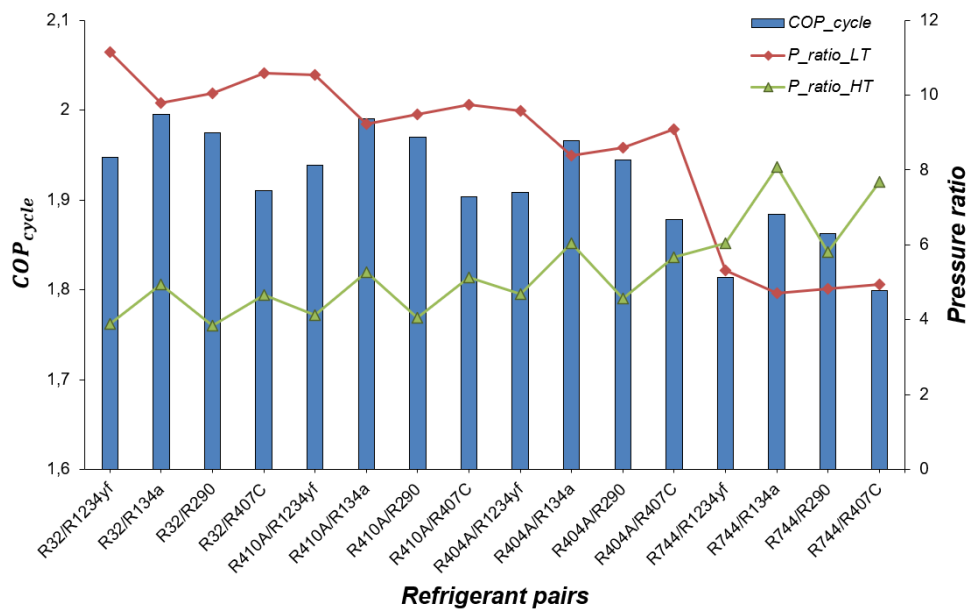


**Figure 11.**  $COP_{cycle}$  and pressure ratio obtained for  $T_{amb} = -30\text{ }^{\circ}\text{C}$ .

As mentioned above, in refrigeration and heat pump technology industry, a compression ratio of not more than 9-10 is recommended to prevent compressor breakdown and efficient system operation [TSO 18]. Due to this limitation in pressure ratio the temperature range between  $T_{amb}$  and  $T_{del}$  is also limited. Figs. 11 and 12 shows  $COP$ ,  $f_q$  chart and pressure ratios for these refrigerants' pairs.

For all refrigerant pairs, except when R744 is used as first refrigerant, the compressor of the low-temperature circuit operates at the maximum limit since the compression ratio  $P_{ratio-LT}$  is close to 10 according to Fig. 11. Since R744 has a highest critical pressure (see Table 1), this allows the first compressor to operate at a lower load in the specified temperature range, with  $P_{ratio-LT}$  around 6. The compression ratio  $P_{ratio-HT}$  for the high-temperature cycle is lower than for the low-temperature cycle for all refrigerant's pairs except those with R744. In this case,  $P_{ratio-HT}$  is in the range from 6 to 9, where 6 is obtained when R290 is used. For refrigerant pairs with R744,  $P_{ratio-HT}$  is higher than  $P_{ratio-LT}$  since  $\text{CO}_2$  refrigerant critical pressure is 1.49 – 1.97 times higher than the other refrigerants according to Table 1.

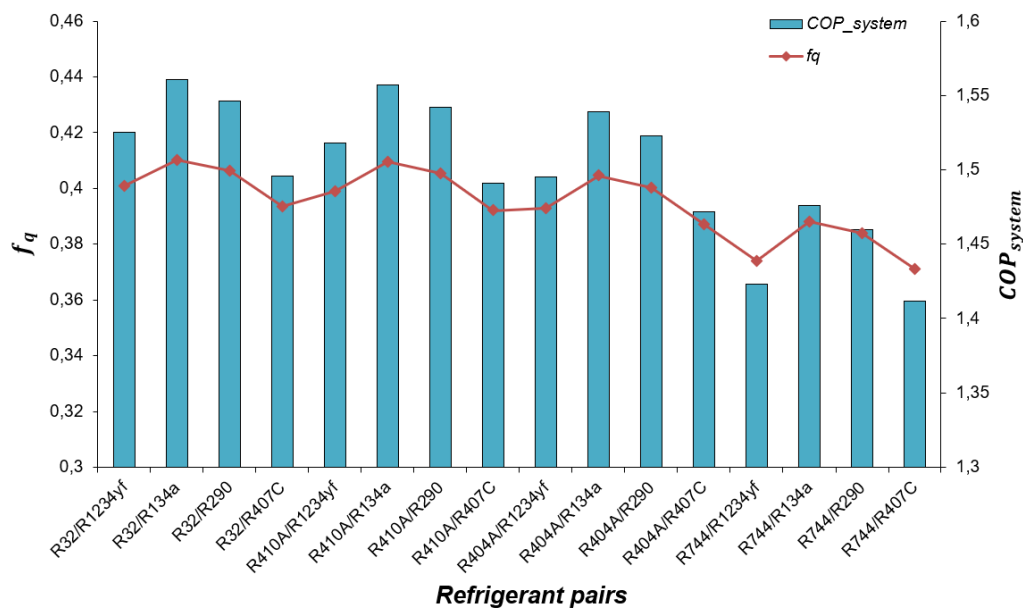


**Figure 12.**  $f_q$  and  $COP_{system}$  obtained for  $T_{amb} = -30\text{ }^{\circ}\text{C}$ .

From the ecological point of view, there are certain limitations on the future use of these refrigerants. Following the results of the Montreal Protocol (1987), measures have been taken to protect the ozone layer and to reduce the use of substances that deplete the ozone layer. With respect to these measures, all refrigerants pairs displayed in Table 1 have zero ODP. It is followed by the Kyoto Protocol (1997), which obliges developed countries and countries with transitional economies to reduce or stabilize greenhouse gas emissions. The recent Paris Agreement (2016) focused on reducing carbon dioxide in the atmosphere and keeping global average temperatures rising below  $+2\text{ }^{\circ}\text{C}$ . According to this last agreement, restrictions on the use of high GWP refrigerants should have been enforced starting from 2020. According to Table 1, restrictions on R404A (GWP=3750), R410A (GWP=1890), R407C (GWP=1700) and R134a (GWP=1410) refrigerants will introduced first. In this respect, synthetic refrigerants such as R32 (GWP=550), R1234yf (GWP=4), and natural refrigerant R744 (GWP=1), hydrocarbon R290 (GWP=20) are being offered in the field of refrigeration, heat pumps and the chemical industry.

Lubricant compatibility between certain refrigerants and refrigerants mixture is also a key factor during retrofitting with new generation refrigerants [MOH 18]. For example, when replacing R22 with refrigerants of the previous generation in accordance with the Montreal Protocol (on the replacement of chlorine-containing refrigerants), R407C and R410A were not miscible with mineral oil. Hence, for HFC refrigerants in current usage such as R134a, R407C and R410A, synthetic lubricant (polyol-ester) is recommended [MOH 18]. In addition, mutual solubility of oil with refrigerants has a significant impact on the characteristics and operation of the heat pump (refrigeration machine) and compressor – heating capacity, energy performance, compressor start/stop characteristics, heat exchangers, oil circulation, compressor reliability. These studies may be carried out in the future for the next generation refrigerants that meet the requirements of the Paris Protocol.

According to these restrictions and the calculations we have presented above, the R32/R290 pair represents a promising solution for future cascade air source heat pumps. However, R32/R290 can only be proposed as interim solution, because it still has a relatively high GWP (550). As a result, it can be concluded that from both environmental friendliness and performance (COP) point of views, the pair R744/R290 is the most suitable among all the pairs we have proposed, because it gives the lowest compression ratio and yields a reasonable COP. However, working with these refrigerants requires new standards, resistant materials, and procedures for operating such working fluids with high pressure and flammability.

## 5. Conclusions

The thermal performances of a cascade “Air-to-Water” heat pump water heater have been numerically investigated with the EES engineering software. The following major conclusions can be drawn from this study:

- R32/R134a and R410A/R134a shows the highest vapor compression cycle  $COP$  1.98 and 3.08 at  $-30\text{ }^{\circ}\text{C}$  and  $+10\text{ }^{\circ}\text{C}$  ambient air temperature, respectively.
- As an environmentally friendly alternative to the above two pairs, the R32/R290 and R744/R290 pairs are proposed.
- The use of R744 and R290 refrigerants allows the compressors to operate at a lower pressure ratio.

Further research on the proposed system includes:

- Cascade system optimal operation control algorithm.
- Cascade heat pump components and overall system thermodynamic optimization.
- Study of intermediate cascade heat exchanger operational conditions.
- Energy and exergy study.

## Acknowledgements

This research is supported by the Ministry of Education and Science of the Republic of Kazakhstan Project AP08857319 “Study of heat transfer enhancement mechanisms of vertical type borehole heat exchanger to ensure high heat pump performance” and the Postdoctoral Research Programme, Al-Farabi Kazakh National University, Almaty, Kazakhstan. The calculations were carried out with the support of the Campus France grant for postdoctoral research by the French Embassy in Kazakhstan (3-month internship).

## Nomenclature

$Q$	Heat Flux (W)
$\dot{m}$	Mass flow rate (kg/s)
$h$	Specific enthalpy (kJ/kg)
$W$	Compressor energy consumption (W)
$T$	Temperature ( $^{\circ}\text{C}$ )
$P$	Pressure (Pa)

## Greek Symbols

$\eta$	Efficiency (-)
--------	----------------

## Subscripts

evap	Evaporator
comp	Compressor
cond	Condenser
ref	Refrigerant
vol	Volumetric
motor	Motor
LT	Low temperature
HT	High temperature
1, 5	Compressor suction/evaporator outlet
2, 6	Compressor discharge/condenser inlet

3, 7	Condenser outlet/expansion device inlet
4, 8	Expansion device outlet/evaporator inlet
total	Total power consumption
overall	Overall COP

## Abbreviation

COP	Coefficient of Performance
CAT	Closest Approach Temperature
EES	Engineering Equation Solver
GWP	Global Warming Potential
ODP	Ozone Depletion Potential

## Bibliography

- [YER 20] Yerdesh Ye., Abdulina Z., Aliuly A., Belyayev Ye., Mohanraj M., Kaltayev A. «Numerical simulation on solar collector and cascade heat pump combi water heating systems in Kazakhstan climates», *Renewable Energy*, 145, p. 1222-1234, 2020.
- [BOA 21] Boahen S., Anka S.K., Lee K.H., Choi J.M. «Performance characteristics of a cascade multi-functional heat pump in the winter season», *Energy and Buildings*, 253, 111511, 2021.
- [LI 21] Li R., Zhu Y., Yang Y., Li K., Zhang R., Sun J., Sun Z. «The effects of the opening of the electronic expansion valve in the high-stage cycle on the performance of a cascade heat pump water heater», *Journal of Building Engineering*, 42, 103015, 2021.
- [ZOU 20] Zou H., Li X., Tang M., Wu J., Tian C., Butrymowicz D., Ma Y., Wang J. «Temperature stage matching and experimental investigation of high-temperature cascade heat pump with vapor injection», *Energy*, 212, 118734, 2020.
- [WU 21] Wu Z., Wang X., Sha L., Li X., Yang X., Ma X., Zhang Y. «Performance analysis and multi-objective optimization of the high-temperature cascade heat pump system», *Energy*, 223, 120097, 2021.
- [ZHA 21] Zhang H., Geng X., Shao S., Si C., Wang Z. «Performance analysis of a R134a/CO<sub>2</sub> cascade heat pump in severe cold regions of China», *Energy*, 122651, 2021.
- [LE 19] Le K. X., Huang M. J., Shah N. N., Wilson C., Artain P. M., Byrne R., Hewitt N. J. «Techno-economic assessment of cascade air-to-water heat pump retrofitted into residential buildings using experimentally validated simulations», *Applied Energy*, 250, p. 633-652, 2019.
- [YAN 21] Yang, L. W., Xu R. J., Xua N., Xia Y., Zhou W. B., Yang T., Belyayev Ye., Wang H. S. «Review of the advances in solar-assisted air source heat pumps for the domestic sector», *Energy Conversion and Management*, 247, 114710, 2021.
- [EES 18] EES - Engineering Equation Solver, Professional Version 10.538, F-Chart Software (2018).
- [MOH 18] Mohanraj M., Belyayev Ye., Jayaraj S., Kaltayev A. «Research and developments on solar assisted compression heat pump systems - A comprehensive review (Part A: Modeling and modifications)», *Renewable and Sustainable Energy Reviews*, 83, p. 90-123, 2018.
- [MOH 18] Mohanraj M., Belyayev Ye., Jayaraj S., Kaltayev A. «Research and developments on solar assisted compression heat pump systems - A comprehensive review (Part-B: Applications)», *Renewable and Sustainable Energy Reviews*, 83, p. 124-155, 2018.
- [TRU 10] Trubayev P., Grishko B. «Heat Pumps: Tutorial», Belgorod BSTU publisher, 143, 2010. Book in Russian.
- [SOK 81] Sokolov Ye. Ya., Brodyanskiy B. M. «Energy fundamentals of heat transformation and cooling processes», *Textbook for universities. - 2nd ed., Revised, Moscow: Energoizdat Publisher*, p. 320, 1981. Book in Russian.
- [KOS 85] Koshkin N. N., Sakun I. A., Bambushek Ye. M., Buharin N. N., Gerasimov Ye. D., Ilyin A. Ya., Pekarev V. I., Stukalenko A. K., Timofyevskiy L. S. «Refrigeration machines and installations», *Textbook for technical colleges*, Leningrad: Mechanical Engineering Publisher, p. 510, 1985. Book in Russian.
- [KIM 14] Kim D. H., Kim M. S. «The effect of water temperature lifts on the performance of cascade heat pump system», «*Applied Thermal Engineering*», 67, p. 273-282, 2014.
- [SON 17] Song Y., Li D., Cao F., Wang X. «Theoretical investigation on the combined and cascade CO<sub>2</sub>/R134a heat pump systems for space heating», *Applied Thermal Engineering*, 124, p. 1457–1470, 2017.

- [FEI 18] Feidt M. «Finite Physical Dimensions Optimal Thermodynamics I-II», Elsevier ISTE Press Ltd 2018. Book in two editions. ISBN 978-1-78548-233-5. Ed. I - P.214 and Ed. II - P.194, 2018. Book available in French.
- [MA 17] Ma X., Zhang Y., Li X., Zou H., Deng N., Nie J., Yu X., Dong S., Li W. «Experimental study for a high efficiency cascade heat pump water heater system using a new near-zeotropic refrigerant mixture», *Applied Thermal Engineering*, 2017.
- [HVA 19] «State regulations in the field of architecture, construction, and urban planning», *Set of rules of the Republic of Kazakhstan. HVAC*, SR RK 4.02-101-2012\*. Nur-Sultan, 2019.
- [TSO 12] Tsoi A., Kim I. «Refrigeration Technology and Cold Consumer Technology: Tutorial», “SK-print” LLP Publisher. ISBN 978-601-263-174-6. Almaty, 2012 (Book available in Kazakh/Russian).